Current Biology, Volume *24*

Supplemental Information

Tension-Sensitive Actin Assembly Supports Contractility at the Epithelial Zonula Adherens

Joanne M. Leerberg, Guillermo A. Gomez, Suzie Verma, Elliott J. Moussa, Selwin K. Wu, Rashmi Priya, Brenton D. Hoffman, Carsten Grashoff, Martin A. Schwartz, and Alpha S. Yap

Figure S1:

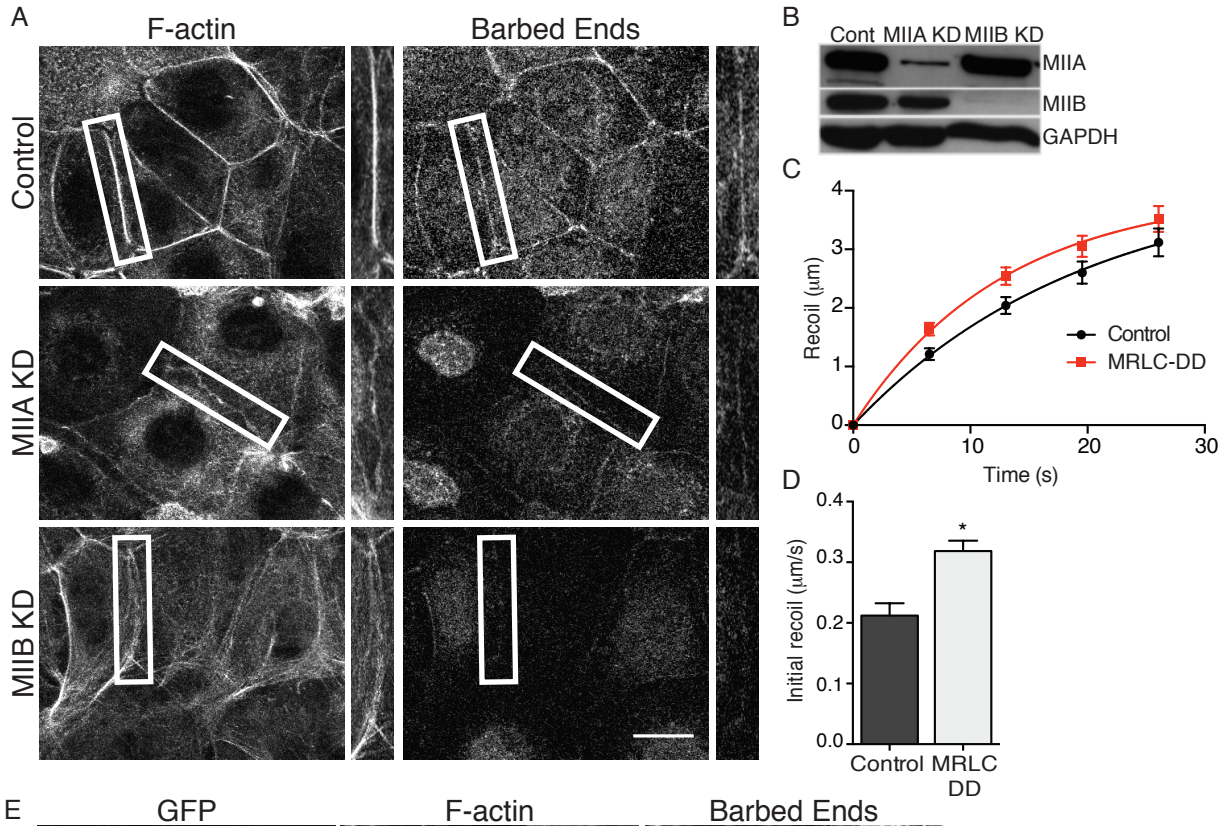
A
F-actin
Barbed Ends
Control
MIIA KD
MIIB KD
B
Cont MIIA KD MIIB KD
MIIA
MIIB
GAPDH
C
Recoil (μm)
Time (s)
Control
MRLC-DD
D
Initial recoil (μm/s)
Control
MRLC DD
*

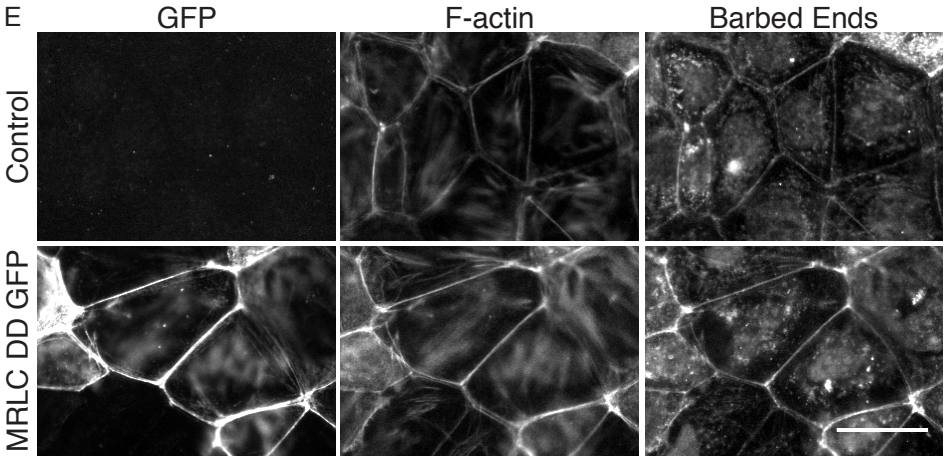
E
GFP
F-actin
Barbed Ends
Control
MRLC DD GFP

Figure S2:

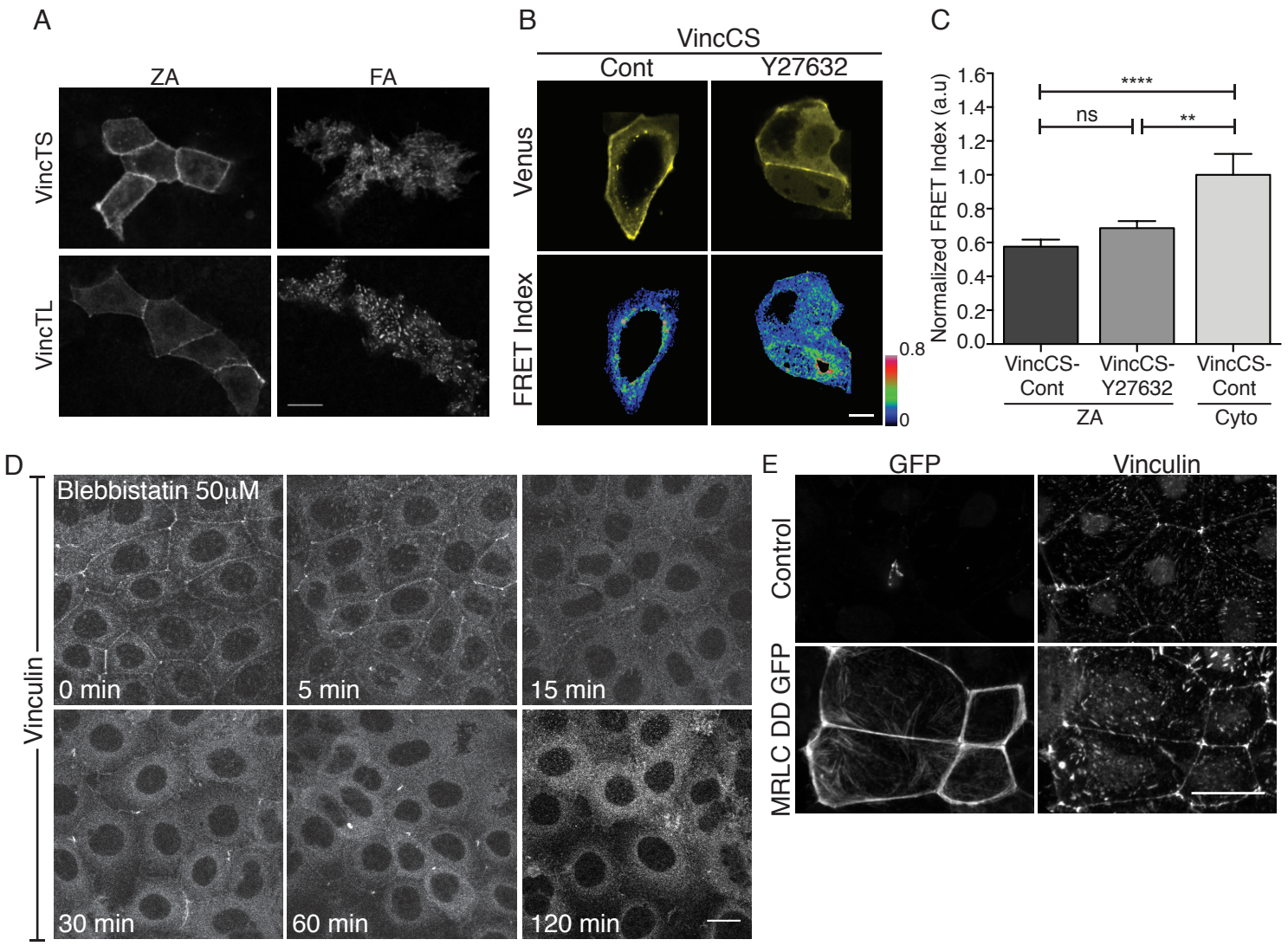
A
ZA
FA
VincTS
VincTL
B
VincCS
Cont
Y27632
Venus
FRET Index
0.8
0
C
Normalized FRET Index (a.u)
1.6
1.4
1.2
1.0
0.8
0.6
0.4
0.2
0.0
****
ns
**
VincCS-Cont
VincCS-Y27632
VincCS-Cont
ZA
Cyto
D
Blebbistatin 50μM
Vinculin
0 min
5 min
15 min
30 min
60 min
120 min
E
GFP
Vinculin
Control
MRLC DD GFP

Figure S3:

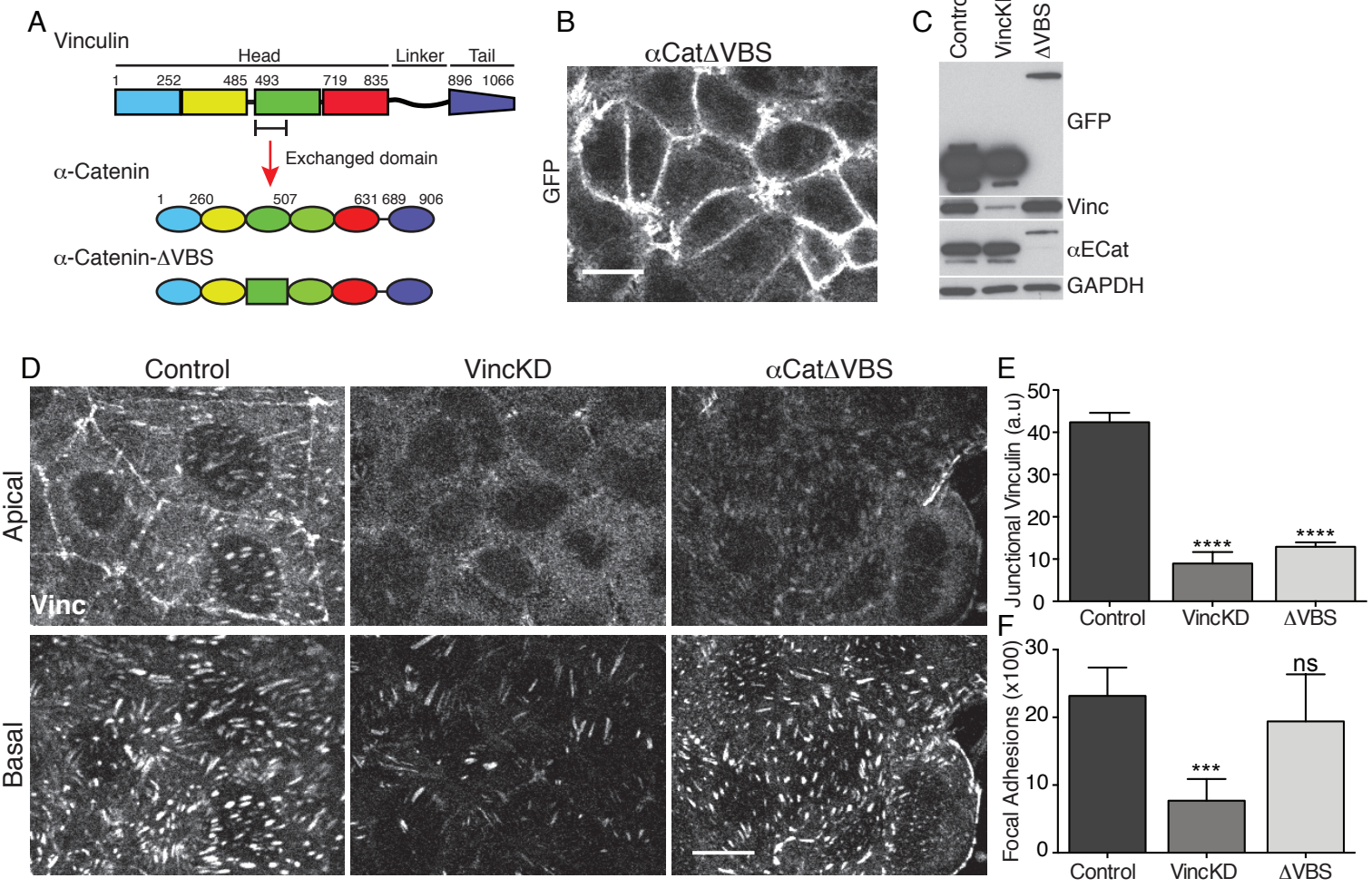
A
Vinculin
Head
Linker
Tail
1
252
485
493
719
835
896
1066
Exchanged domain
α-Catenin
1
260
507
631
689
906
α-Catenin-ΔVBS
B
αCatΔVBS
GFP
C
Control
VincKD
ΔVBS
GFP
Vinc
αECat
GAPDH
D
Control
VincKD
αCatΔVBS
Apical
Basal
Vinc
E
Junctional Vinculin (a.u)
50
40
30
20
10
0
****
****
Control
VincKD
ΔVBS
F
Focal Adhesions (x100)
30
20
10
0
***
ns
Control
VincKD
ΔVBS

Figure S4:

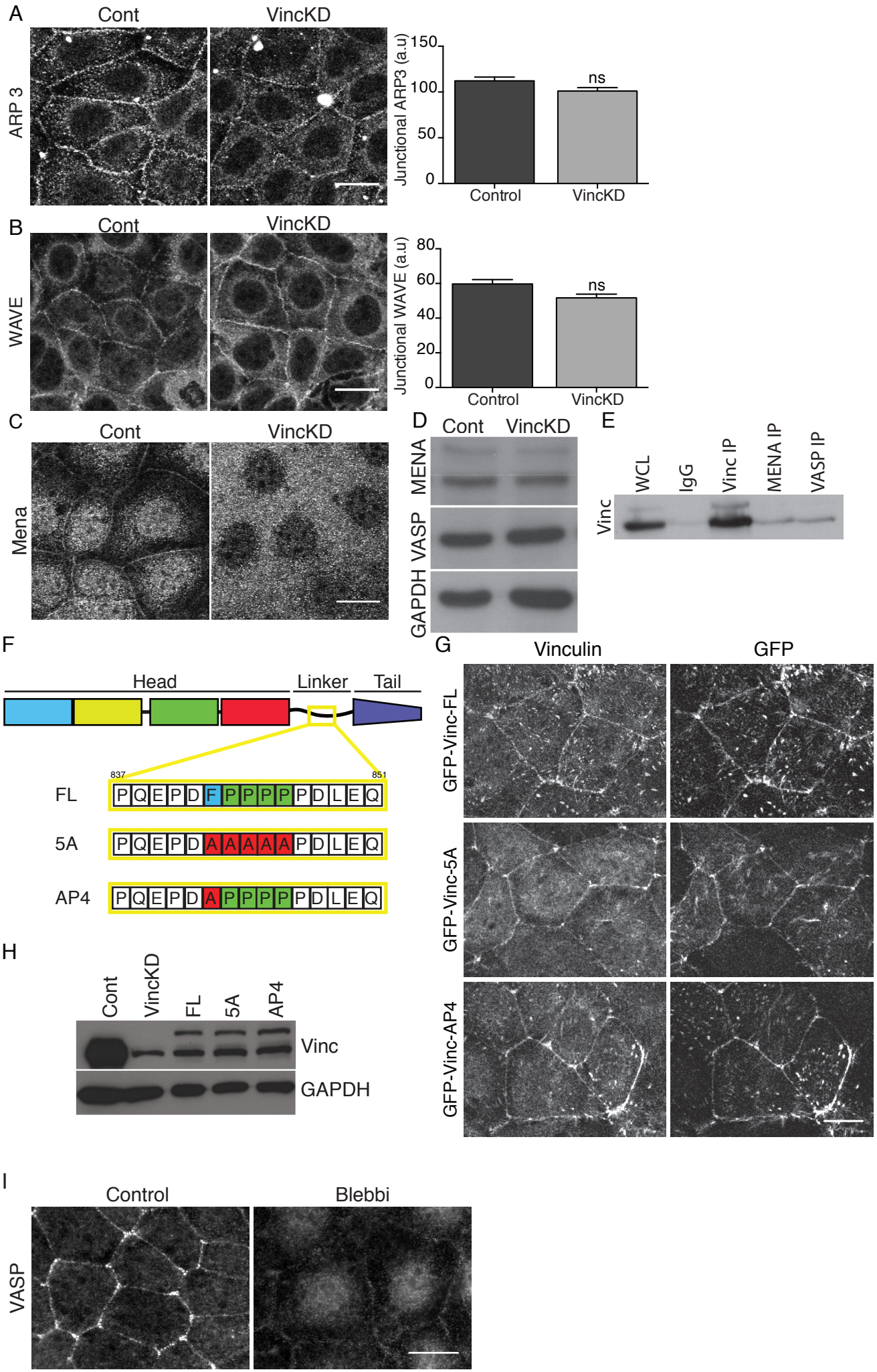
A
Cont
VincKD
ARP 3
Junctional ARP3 (a.u)
150
100
50
0
ns
Control
VincKD
B
Cont
VincKD
WAVE
Junctional WAVE (a.u)
80
60
40
20
0
ns
Control
VincKD
C
Cont
VincKD
Mena
D
Cont
VincKD
MENA
VASP
GAPDH
E
WCL
IgG
Vinc IP
MENA IP
VASP IP
Vinc
F
Head
Linker
Tail
837
851
FL
P Q E P D F P P P P P D L E Q
5A
P Q E P D A A A A A P D L E Q
AP4
P Q E P D A P P P P P D L E Q
G
Vinculin
GFP
GFP-Vinc-FL
GFP-Vinc-5A
GFP-Vinc-AP4
H
Cont
VincKD
FL
5A
AP4
Vinc
GAPDH
I
Control
Blebbi
VASP

Figure S5

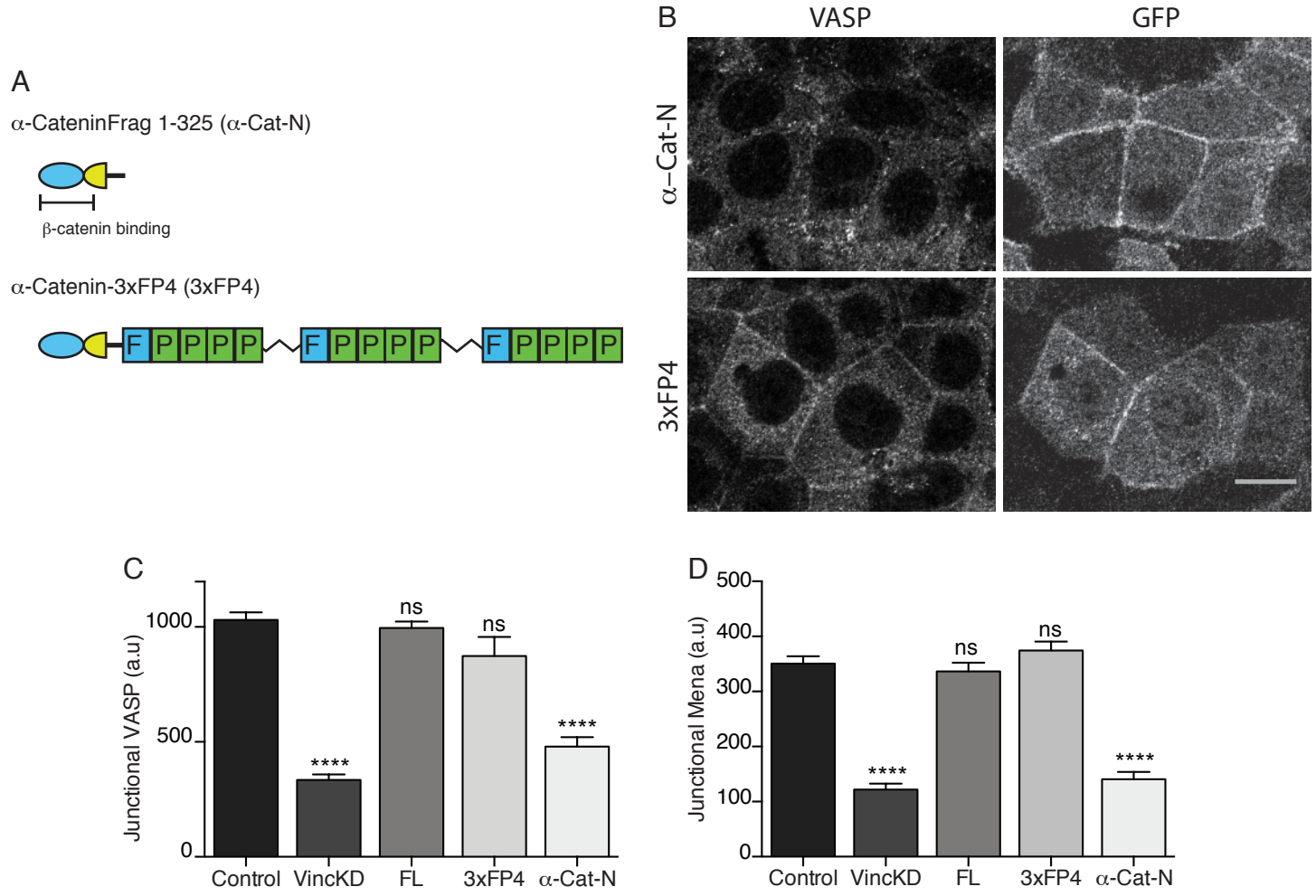
A
α-CateninFrag 1-325 (α-Cat-N)
β-catenin binding
α-Catenin-3xFP4 (3xFP4)
F P P P P F P P P P F P P P P
B
VASP
GFP
α–Cat-N
3xFP4
C
Junctional VASP (a.u)
1000
500
0
ns
ns
****
****
Control
VincKD
FL
3xFP4
α-Cat-N
D
Junctional Mena (a.u)
500
400
300
200
100
0
ns
ns
****
****
Control
VincKD
FL
3xFP4
α-Cat-N

Supplementary Figure Legends

Figure S1 (related to Figure 1). Manipulations of junctional tension.

A) Representative images of F-actin (phalloidin) and barbed-end labelling (G-actin incorporation) at the apical junctions of control, Myosin IIA shRNA and Myosin IIB shRNA cells. Rectangles mark detailed junctional regions shown on the right side of each panel. Scale bar: 20μm.

B) Western blot analysis of myosin IIA and myosin IIB expression in control, Myosin IIA shRNA or Myosin IIB shRNA Caco-2 cell lines. GAPDH was used as a loading control.

C,D) Junctional tension measured by laser nanoscissors of apical junctions. Recoil curves (C) and initial recoil velocity (D); Data are means ± SEM of n=3 (biological replicates). *P<0.05; compared with control; Nonlinear Regression, One-phase association and Student's t-test.

E) Representative images of F-actin and barbed-end labelling at the apical junctions of cells transfected with GFP (control) or MRLC-DD-GFP. Note that soluble GFP is substantially lost by the permeabilisation of live cells that is required for G-actin labelling. Scale bar equals 20μm.

Figure S2 (related to Figure 2). Vinculin conformation sensor and localisation of junctional vinculin in tension manipulated cells.

A) Localisation of VincTS and VincTL to the ZA and focal adhesions within cells.

B,C) Vinculin conformation at the ZA and cytosol. FRET index images (B) and quantitation (C) for vinculin conformation (VincCS) within the cytosol or at the ZA in the presence or absence of Y27632. Data are mean ± SEM for at least 60 images per condition pooled from 4 independent experiments. ns, not significant; **P<0.01; ****P<0.0001; One-way ANOVA, Sidak's multiple comparison test.

D) Representative images of vinculin at the apical junctions of cells treated with 50μM blebbistatin and fixed at the time indicated.

E) Representative images of control and MRLC-DD expressing cells showing GFP and vinculin localisation. Scale bar: 20μm.

Figure S3 (related to Figure 3). Alpha-catenin-ΔVBS mutant selectively depletes junctional vinculin.

A) Schematic representation of vinculin and α-catenin showing domain swap to create α-catenin-ΔVBS mutant. Modified from Choi et al. (2012) and Huveneers et al. (2012).
B) α-catenin-ΔVBS-GFP localisation to contact in Caco-2 infected and FACS sorted cells. Scale bar: 20μm.
C) Western blot analysis of lysed cells. Lane 1 control, lane 2 stably generated vinculin knockdown (VincKD) and lane 3 stably generated α-catenin-ΔVBS mutant (ΔVBS) expressed in siRNA α-catenin cells.
D) Apical and basal confocal sections from control, vinculin knockdown and α-catenin-ΔVBS mutant (depleted of endogenous α-catenin) cells, fixed and stained with vinculin.
E) Peak vinculin content at the contacts as measured by line scan. Data are representative of 50 contacts pooled from 3 individual experiments, (**** $P < 0.0001$; One-way ANOVA, Dunnett's post hoc test).
F) Number of focal adhesions as determined by spot counting (ImageJ, 1.47i). Data are representative of 15 fields of view from 3 independent experiments (*** $P < 0.001$, ns, not significant; One-way ANOVA, Dunnett's post hoc test).

Figure S4 (related to Figure 4). Vinculin and junctional Mena/VASP.
A) Representative images of control and vinculin shRNA knockdown cells (VincKD) showing Arp3 localisation at junctions, with line scan quantification showing no significant change.
B) Representative images of control and vinculin shRNA knockdown cells (VincKD) showing WAVE localisation at junctions, with line scan quantification showing no significant change.
C) Representative images of control and vinculin shRNA knockdown cells (VincKD) showing Mena localisation at junctions.
D) Western blot analysis of total cellular levels of Mena and VASP for control and vinculin shRNA knockdown (VincKD) cells. GAPDH was used at a loading control.
E) Immunoprecipitation of vinculin, Mena and VASP blotted back with an antibody against vinculin. IgG was used as a negative control. Representative of three individual experiments.
F) Schematic representation of full-length vinculin highlighting the Mena/VASP binding domain (FP4).

G) Representative images of vinculin full-length and Mena/VASP uncoupled mutants vinc-5A and Vinc-AP4 (expressed in VincKD cells) showing GFP expression and vinculin localisation.

H) Western blot analysis of whole cell lysate of control, vinculin knockdown (VincKD), and vinculin knockdown reconstituted with either full-length vinculin, vinc-5A or vinc-AP4 mutants.

I) Representative image of junctional localisation of VASP in Caco-2 cells in the presence or absence of 50μM blebbistatin.

Scale bar equals 20μm. Data representative of 3 biological replicates. ns, not significant; Student's t-test.

Figure S5 (related to Figure 5). Membrane targeted FP4 domain rescues junctional Mena/VASP in vinculin depleted cells.

A) Schematic representation of α-catenin fragment (1-325) and α-catenin-3xFP4.

B) Immunofluorescent staining of PFA fixed cells stained with anti-VASP and anti-GFP antibodies. Scale bar equal 20μm. Peak junctional content of (C) VASP and (D) Mena determined by line scan analysis (**** $P > 0.0001$; ns, not significant; One-way ANOVA, Dunnett's post hoc test). Data is representative of 50 contacts pooled from 3 individual experiments.

Supplementary Experimental Procedures.

Transfection and siRNA knockdown

Cells were transfected using Lipofectamine 2000 (Invitrogen) for expression constructs according to the manufacturer's instructions and analysed 24-48 h after transfection. Lipofectamine RNAiMAX (Invitrogen) was used to deplete human α-Catenin using a 'double hit' approach. Briefly, 5 μl of Lipofectamine RNAiMAX was added to 250 μl of OptiMEM (Gibco) and incubated at RT for 5 min. This was added to 0.25 μM of α-Catenin siRNA (On-Targetplus SMARTpool; J-010505-06; CTNNA1; GAUGGUAUCUUGAAGUUGA; Dharmacon) and made up to 500 μl with OptiMEM. The Lipofectamine/DNA solution was incubated for 20 min at RT. The volume of this solution was increased to 2 mL with OptiMEM with 10% FBS. The cells were incubated at 37 °C for 8 h, before the media was replaced with RPMI (supplemented with 10% FBS-HI, 1% NEAA, 1% L-glutamine, 100 Units/mL Penicillin, 100 Units.ml Streptomycin). The cells were incubated at 37 °C for a further 24 h before being trypsinised and plated at 30-40% confluency directly onto either a 35 mm dish or onto coverslips and incubated for a further 24 h. The second round of siRNA transfection was repeated after which the cells were incubated for 36-48 h.

Plasmids and shRNA reagents

A lentivirus-based system [S1, S2] was used to functionally silence vinculin in mammalian cells. The lentivirus expression vector pLL5.0 (backbone pLL3.7) and the third-generation packaging constructs pMDLg/pRRE, RSV-Rev and pMD.G were gifts from J.E. Bear (UNC Chapel Hill, North Carolina USA). shRNA sequences targeted against human-vinculin were designed according to the requirements for effective RNAi and the specific requirements of the lentiviral expression vector (5'-GGATGTGCTCACAGCAAAA-3') [S1, S3]. The shRNA was cloned downstream of the U6 promoter (HpaI and XhoI) into pLL5.0 carrying either soluble or NLS-eGFP or mCherry as reporter genes driven from an LTR promoter. The pLL5.0 and packaging vectors were transfected into HEK-293T cells by either $CaCl_2$ precipitation or lipid transfection. 16 h after transfection, cells were treated with sodium butyrate (10 mM) to increase gene induction. Virus-like particles (VLPs) were harvested from the supernatant 48-72 h after transfection and concentrated on poly(vinylidene difluoride) spin columns (Millipore) to obtain high titres of VLP fractions.

Caco-2 cells were incubated at 37 °C with lentiviral particles in cRPMI and polybrene solution (8 μg/mL) and harvested by trypsinisation 72 h after infection. Single-cell suspensions were sorted by flow cytometry according to the high levels of the reporter gene expression. Knockdown was determined by Western Blot analysis.

Full-length mouse-vinculin [S4] was amplified by PCR and cloned into pEGFP-C1 (Clontech) via the EcoRI site. α-E-Catenin Frag (aa residues 1-325) was amplified and cloned into pEGFP-C1 via the BglII and HindIII restriction sites. Triple FP4 was synthesised (Integrated DNA Technologies) as sense (/5Phos/CTGAAGCTTCG AATTCCTTCCCGCCTCCTCCATCTGGTTTGTTCCCGCCTCCTCCATCTCGTTTGT TCCCGCCTCCTCCA) and anti-sense (/5Phos/GTCGACTGCAGAATTCGCT GGAGGAGGCGGGAACAAACGAGATGGAGGAGGCGGGAACAAACCAGATGGAG GAGGCGGGAA) sequences, which were then annealed and cloned C-terminally into GFP-Alpha-E-Cat (Frag) via the EcoRI and SalI restriction sites.

The Quick Change II XL Site-directed mutagenesis kit (Integrated Sciences) was used to generate the AP4 and 5A vinculin mutants. Primers were designed as follows: AP4 Sense (5' – CCTCAGGAGCCTGACGCCCCGCCTCCTCCACC – 3') and anti-sense (5' – GGTGGAGGAGGCGGGGCGTCAGGCTCCTGAGG – 3'). 5A sense (5' – CCTCAGGAGCCTGACGCC GCGGCTGCTGCACCAGACCTTGAACAG – 3') and anti-sense (5' – CTGTTCAAGGTCTGGTGCAGCAGCCGCGGCGTCAGGCTC CTGAGG – 3'). The pEGFP-C1 constructs were cloned into pLL5.0 vinculin KD downstream of the LTR promoter.

MRLC-DD (T18D/S19D) [S5] was obtained from Addgene and EGFP-AP4-mito and EGFP-FP4-mito have been previously described [S6]. In experiments where both MRLC-DD and EGFP-AP4-mito or EGFP-FP4-mito expression were required the following constructs were used. MRLC-DD-pIRES-EGFP-AP4-mito and MRLC-DD-pIRES-EGFP-FP4-mito constructs were made by inserting the MRLC-DD fragment downstream of the CMV promoter using the XbaI/XhoI restriction sites and IRES was inserted using the NotI/EcoRI restriction site upstream of the GFP-F(A)P4-mito sequence within the pCDNA3.1(-) backbone.

Antibodies, immunoprecipitation and inhibitors

Primary antibodies used in this study were as follows: (1) mouse monoclonal antibody (mAb) against vinculin (Invitrogen Cat# V-9131); (2) rabbit polyclonal

antibody (pAb) against vinculin (Abcam Cat# ab91459); (3) mouse mAb HECD1 against the ectodomain of E-cadherin (a gift from Dr Wheelock, University of Nebraska, Omaga, NE with the permission of M. Takeichi); (4) rabbit pAb against Mena and (5) rabbit pAb against VASP (gifts from Frank Gertler, Massachusetts Institute of Technology, Cambridge, Massachusetts); (6) rabbit mAb against VASP (9A2) (Cell Signalling Cat#3132); (7) rabbit pAb against α-Catenin (Invitrogen Cat#71-1200); (8) rabbit pAb against Myosin IIA (Covance Cat#PRB-440P); (9) rabbit pAb against Myosin IIB (Covance Cat#PRB-445P);(10) rabbit pAb against WAVE2 (Cell Signalling Technology Cat#D2C8); (11) mouse mAb against Arp3 (Sigma Cat#HPA02446711); (12) rabbit pAb against GAPDH (Bio-Scientific – RDS Cat#2275); (13) mouse mAb against GFP (Molecular Probes Cat#A-11120); (14) chicken pAb against GFP (Sapphire Bioscience – Abcam Cat#ab13970). F-actin was stained with AlexaFluor 488-, 546-, 594-, 647-phalloidin (1:1,000 dilution; Invitrogen). Secondary antibodies were species-specific antibodies conjugated with AlexaFluor 488, 546, 594 or 647 (Invitrogen) for immunofluorescence, or with horseradish peroxidase (Bio-Rad Laboratories) for immunoblotting.

Caco-2 cells were plated onto two 15 cm dishes per immunoprecipitation and grown to confluence. Cells were lysed in 1 mL of lysis buffer (50 mM Tris [pH 7.4], 2 mM $CaCl_2$, 150 mM NaCl, 0.5% NP40). Protein complexes were immunoprecipitated with antibody bound to protein A –agarose beads and were separated by SDS-PAGE.

Caco-2 cells were seeded at 30-40% confluency onto coverslips and allowed to recover to 80-90% confluency before drug treatment. Cells were treated with Blebbistatin (Merck Cat# US1203390) at a final concentration of 50 µM for 2 hours or Y27632 (Merck Cat# 688000) at a final concentration of 100 µM for 3 hours.

Supplementary References

S1. Rubinson, D.A., Dillon, C.P., Kwiatkowski, A.V., Sievers, C., Yang, L., Kopinja, J., Rooney, D.L., Zhang, M., Ihrig, M.M., McManus, M.T., et al. (2003). A lentivirus-based system to functionally silence genes in primary mammalian cells, stem cells and transgenic mice by RNA interference. Nat. Genet. *33*, 401-406.

S2. Vitriol, E.A., Uetrecht, A.C., Shen, F., Jacobson, K., and Bear, J.E. (2007). Enhanced EGFP-chromophore-assisted laser inactivation using deficient cells rescued with functional EGFP-fusion proteins. Proc. Natl. Acad. Sci. U. S. A. *104*, 6702-6707.

S3. Reynolds, A., Leake, D., Boese, Q., Scaringe, S., Marshall, W.S., and Khvorova, A. (2004). Rational siRNA design for RNA interference. Nat. Biotechnol. *22*, 326-330.

S4. Xu, W., Coll, J.L., and Adamson, E.D. (1998b). Rescue of the mutant phenotype by reexpression of full-length vinculin in null F9 cells; effects of cell locomotion by domain deleted vinculin. J. Cell Sci. *111*, 1535-1544.

S5. Beach, J.R., Licate, L.S., Crish, J.F., and Egelhoff, T.T. (2011). Analysis of the role of Ser1/Ser2/Thr9 phosphorylation on myosin II assembly and function in live cells. BMC Cell Biol. *12*, 52.

S6. Scott, J.A., Shewan, A.M., den Elzen, N.R., Loureiro, J.J., Gertler, F.B., and Yap, A.S. (2006). Ena/VASP proteins can regulate distinct modes of actin organization at cadherin-adhesive contacts. Mol. Biol. Cell *17*, 1085-1095.